

Cover Page



Universiteit Leiden



The handle <http://hdl.handle.net/1887/19115> holds various files of this Leiden University dissertation.

**Author:** Sousa Sánchez, Kepa

**Title:** Consistent supersymmetric decoupling in cosmology

**Date:** 2012-06-20

---

## Conventions.

---

In this thesis we use the units  $c = \hbar = 1$ . Thus, the Plank mass  $m_{pl}$  is simply given by

$$m_{pl}^{-2} \equiv \frac{G}{\hbar c} = G, \quad (\text{A.0.1})$$

where  $G$  is the Newtons constant. In general we will work in units of the reduced Plank mass  $M_p$ ,

$$M_p^{-2} = 8\pi G = 1, \quad (\text{A.0.2})$$

except in applications to cosmology where we might choose to keep  $M_p$  or  $G$  explicitly for clarity.

The use of indices is summarized in table A.1.

### A.1 Space-time conventions

We choose the Minkowski space-time metric  $\eta_{mn}$  to have mostly positive Lorentz signature

$$\eta_{mn} = \text{Diag}(-1, 1, 1, 1). \quad (\text{A.1.1})$$

The Levi-Civita tensor is defined to be totally antisymmetric with  $\varepsilon_{0123} = +1$ .

Space-time indices		
$\mu$	$0, \dots, 3$	space-time coordinates, with $x^0$ for the time
$m$	$0, \dots, 3$	local frame
Supersymmetric truncations in $\mathcal{N} = 1$ supergravity (Chapt. 2-5)		
$I$	$1, \dots, n_C$	chiral multiplets
$\alpha$	$1, \dots, n_h$	truncated chiral multiplets
$i$	$1, \dots, n_l$	surviving chiral multiplets
$a$	$1, \dots, n_V$	vector multiplets
$\tilde{a}$	$1, \dots, \tilde{n}_V$	truncated vector multiplets
$\mathcal{N} = 2$ supergravity (Chapt. 6-7)		
$s$	$1, \dots, n_H$	hypermultiplets
$X$	$1, \dots, 4n_H$	scalar fields in hypermultiplets
$A$	$1, \dots, 2n_H$	spinors in hypermultiplets
$\Lambda$	$0, \dots, n_V$	vector multiplets
$\alpha$	$1, \dots, n_V$	scalar fields and spinors in vector multiplets
$i$	$1, 2$	SU(2)
$x$	$1, 2, 3$	triplet of SU(2)

*Table A.1 – Summary of indices.*

Defining the space-time vielbein as

$$g_{\mu\nu} = e_\mu{}^m \eta_{mn} e_\nu{}^n, \quad (\text{A.1.2})$$

the spin connection and the Levi-Civita connection are given by

$$\begin{aligned} \omega_\mu{}^{mn}(e) &= 2e^{\nu[m} \partial_{[\mu} e_{\nu]}{}^n] - e^{\nu[m} e^{n]\sigma} e_{\mu p} \partial_\nu e_\sigma{}^p, \\ \Gamma_{\mu\nu}^\rho &= \frac{1}{2} g^{\rho\lambda} (2\partial_{(\mu} g_{\nu)\lambda} - \partial_\lambda g_{\mu\nu}). \end{aligned} \quad (\text{A.1.3})$$

Both formulations are equivalent due to the constraint

$$\nabla_\mu e_\nu{}^m = \partial_\mu e_\nu{}^m + \omega_\mu{}^{mn}(e) e_{\nu n} - \Gamma_{\mu\nu}^\rho e_\rho{}^m = 0. \quad (\text{A.1.4})$$

The covariant derivative of a vector reads

$$\nabla_\mu k^m = \partial_\mu k^m + \omega_\mu{}^{mn} k_n. \quad (\text{A.1.5})$$

The Ricci tensor can be obtained using the following formulae

$$\begin{aligned} R_{\mu\nu}{}^{mn} &= 2\partial_{[\mu} \omega_{\nu]}{}^{mn}(e) + 2\omega_{[\mu}{}^{mp}(e) \omega_{\nu]p}{}^n(e), \\ R^\mu{}_{\nu\rho\sigma} &= R_{\rho\sigma}{}^{mn} e_m{}^\mu e_{\nu n} = 2\partial_{[\rho} \Gamma_{\sigma]\nu}^\mu + 2\Gamma_{\tau[\rho}^\mu \Gamma_{\sigma]\nu}^\tau, \\ R_{\mu\nu} &= R_{\mu\rho}{}^{nm} e_n{}^\rho e_{\nu m}, \quad R = g^{\mu\nu} R_{\mu\nu}. \end{aligned} \quad (\text{A.1.6})$$

$$(\text{A.1.7})$$

## A.2 Spinor conventions

For the spinor conventions we follow [94]. The gamma matrices satisfy the relations

$$\gamma_m \gamma_n + \gamma_n \gamma_m = 2\eta_{mn}, \quad [\gamma_m, \gamma_n] \equiv \gamma_{mn}, \quad \gamma_5 \equiv i\gamma_0 \gamma_1 \gamma_2 \gamma_3, \quad \gamma_5^2 = 1. \quad (\text{A.2.1})$$

We define left and right projections by

$$P_L = \frac{1}{2}(1 + \gamma_5), \quad P_R = \frac{1}{2}(1 - \gamma_5), \quad (\text{A.2.2})$$

thus, denoting by  $\epsilon_L$  and  $\epsilon_R$  a left and a right handed chiral spinor respectively, they satisfy

$$P_L \epsilon_L = \epsilon_L, \quad P_R \epsilon_R = \epsilon_R. \quad (\text{A.2.3})$$

The covariant derivative of a fermion is given by

$$\nabla_\mu \epsilon = \partial_\mu \epsilon + \frac{1}{4} \omega_\mu^{mn} \gamma_{mn} \epsilon. \quad (\text{A.2.4})$$

## A.3 SU(2) conventions

The SU(2) vector and matrix representations are related by

$$A_i^j \equiv iA^x (\sigma^x)_i^j, \quad A^x = -\frac{1}{2} \text{tr}(\sigma^x A), \quad (\text{A.3.1})$$

where the indices  $i, j$  run over 1, 2, and the index  $x = 1, 2, 3$ . We use the Pauli matrices

$$\sigma^1 = \begin{pmatrix} 0 & 1 \\ 1 & 0 \end{pmatrix}, \quad \sigma^2 = \begin{pmatrix} 0 & -i \\ i & 0 \end{pmatrix}, \quad \sigma^3 = \begin{pmatrix} 1 & 0 \\ 0 & -1 \end{pmatrix}. \quad (\text{A.3.2})$$

SU(2) indices can be raised or lowered using the Levi-Civita tensor  $\varepsilon_{ij}$

$$\varepsilon_{12} = 1 \quad \varepsilon^{12} = 1, \quad \varepsilon_{ij} \varepsilon^{jk} = -\delta_i^k, \quad (\text{A.3.3})$$

and we contract them using NorthWest-SouthEast convention (NW-SE)

$$A_i = A^j \varepsilon_{ji}, \quad A^i = \varepsilon^{ij} A_j. \quad (\text{A.3.4})$$

In  $\mathcal{N} = 2$  supergravity the R-symmetry is SU(2). Since inside each multiplet, the fields are arranged into representations of the R-symmetry, in particular the fermions are labeled by an SU(2) index. We use the position of the index to denote left or right chirality:

$$P_L \epsilon^i = \epsilon^i, \quad P_R \epsilon_i = \epsilon_i. \quad (\text{A.3.5})$$



---

## Stability of axionic $D$ -term strings.

---

In this appendix we review the work presented in [72] which discusses the stability of a class of BPS solutions appearing in the globally supersymmetric model of Blanco-Pillado *et al.* [59]. The model describes a D-brane anti-D-brane unstable system after compactification to four dimensions, which is relevant for the study of the late stages of the brane antibrane inflationary model.

The cosmic strings appearing in the model were conjectured to be the low energy manifestation of D-strings that might form from tachyon condensation after D- anti-D-brane annihilation in type IIB superstring theory. The model describes the dynamics of two scalar fields, the tachyon and an axio-dilaton field, the later associated to the volume modulus and the Ramond-Ramond field which couples to the D-branes. The model admits three one-parameter families of cylindrically symmetric one-vortex solutions to the BPS equations, which are called tachyonic, axionic and hybrid strings, depending on which field sources the magnetic field in the core of the string. Different vortex solutions within a family have the same energy and varying core radius.

In particular we discuss the dynamics of the zero mode associated to the parameter connecting different string solutions within a family. We use a technique previously applied by R.A. Leese [156] in the case of semilocal strings [155]. We show that axionic strings behave similarly to semilocal strings, i.e.

if the string solution is perturbed, the evolution of the zero mode leads to the spread of the magnetic flux and the eventual disappearance of the string. In a cosmological setting these strings are expected to experience all sorts of perturbations, and therefore they would tend to become wider with time until they vanish.

This analysis is also useful to understand the stability of the cosmic strings found in the  $\mathcal{N} = 2$  supergravity model presented in chapter 7. As in [59] the model admits a family of cosmic string solutions with equal energy and different radii. In section 7.5.3 we argued that the zero mode associated to the parameter connecting different solutions can not be excited by any finite energy perturbation. We will discuss again this statement in connection with the results we review here in the last section of this appendix.

## B.1 The model

The lagrangian proposed in [59] describes a globally supersymmetric abelian Higgs model containing a vector multiplet and two chiral multiplets. One chiral multiplet contains a chiral field  $\phi$  with canonical kinetic terms that represents the tachyon, and the other chiral multiplet involves an axion-dilaton field  $S = s + ia$ . The vector multiplet contains a gauge field denoted by  $A_\mu$ .

As in the case of supergravity, globally supersymmetric models are defined in terms of a Kähler potential, a superpotential, the gauge kinetic functions and the gauge couplings (a review of globally supersymmetric models can be found in [18]). The Kähler potential is given by

$$K = \phi\bar{\phi} - \log(S + \bar{S}), \tag{B.1.1}$$

the superpotential is chosen to be zero,  $W(\phi, S) = 0$ , and the gauge kinetic function is set to be constant,  $f(S) = 1/g^2$ , where  $g$  is the gauge coupling.

The gauge boson,  $A_\mu$ , in the vector multiplet is coupled to the scalar fields gauging a combination of the  $U(1)$  isometry of the tachyon and the shift symmetry of the axio-dilaton system:

$$\delta_{gauge}\phi = iq\phi\chi \quad \delta_{gauge}S = -i2\delta\chi. \tag{B.1.2}$$

where  $q$  is the charge of the tachyon,  $\delta$  is the coupling of the axion to the gauge field, and  $\chi$  is the gauge parameter. Thus the corresponding covariant derivatives are given by:

$$D_\mu\phi = \partial_\mu\phi - iqA_\mu\phi, \quad D_\mu S = \partial_\mu S + i2\delta A_\mu. \tag{B.1.3}$$

In globally supersymmetric models the  $D$ -term potential is obtained from the killing vectors and the Kähler potential using the same expressions as in su-

## B.2. Cosmic string solutions

---

pergravity, (2.2.14) and (2.2.16). This particular model also includes a Fayet-Iliopoulos term  $\xi$ , and therefore the  $D$ -term potential reads:

$$V_D = \frac{1}{2}D^2, \quad D = g(\xi - \delta s^{-1} - |\phi|^2). \quad (\text{B.1.4})$$

The bosonic sector of the lagrangian, after eliminating the auxiliary field from the vector multiplet, is:

$$\mathcal{L} = -D_\mu \phi D^\mu \bar{\phi} - \frac{1}{4}s^{-2} D_\mu S D^\mu \bar{S} - \frac{1}{4}g^{-2} F^{\mu\nu} F_{\mu\nu} - \frac{1}{2}g^2 (\xi - \delta s^{-1} - q|\phi|^2)^2. \quad (\text{B.1.5})$$

where  $F_{\mu\nu} = \partial_\mu A_\nu - \partial_\nu A_\mu$  is the abelian field strength associated to the gauge boson  $A_\mu$ . It is convenient to write the bosonic part of the lagrangian using the rescalings:

$$\phi = \sqrt{\xi/q} \hat{\phi}, \quad s = \delta/\xi \hat{s}, \quad a = 2\delta/q \hat{a}, \quad A_\mu = g\sqrt{\xi/q} \hat{A}_\mu, \quad x = (g\sqrt{\xi q})^{-1} \hat{x}. \quad (\text{B.1.6})$$

With these definitions the axion  $\hat{a}$  is defined modulo  $2\pi$ , and  $\delta$  is rescaled away. After dropping the hats, the bosonic sector of the lagrangian reads:

$$\begin{aligned} \mathcal{L}(\xi g)^{-2} &= -D_\mu \phi D^\mu \bar{\phi} - \frac{1}{4}(\alpha s)^{-2} \partial_\mu s \partial^\mu s - (\alpha/s)^2 (\partial_\mu a + A_\mu)(\partial^\mu a + A^\mu) \\ &\quad - \frac{1}{4}F^{\mu\nu} F_{\mu\nu} - \frac{1}{2}(1 - s^{-1} - |\phi|^2)^2, \end{aligned} \quad (\text{B.1.7})$$

with  $D_\mu \phi = \partial_\mu \phi - iA_\mu \phi$ , and  $\alpha^2 = \xi/q$ . Note that  $\alpha$  is the symmetry breaking scale in Plank units.

## B.2 Cosmic string solutions

To study straight vortices along, say, the  $z$ -direction, we drop the  $z$  dependence and set  $A_z = 0$ . For time independent configurations and defining  $\tilde{S} = s + 2i\alpha^2 a$ , and  $\tilde{D}_\mu \tilde{S} = \partial_\mu \tilde{S} + 2i\alpha^2 A_\mu$ , the energy per unit length can be written in the Bogomolnyi form:

$$\begin{aligned} \mu_{string} &= (\xi g)^2 \int_M d^2x \left( |(D_x \pm iD_y)\phi|^2 + \frac{1}{4}(\alpha s)^{-2} |(\tilde{D}_x \pm i\tilde{D}_y)\tilde{S}|^2 \right. \\ &\quad \left. + \frac{1}{2}(F_{xy} \mp (1 - s^{-1} - |\phi|^2))^2 \pm F_{xy} \right. \\ &\quad \left. \mp i[\partial_x(\phi^* D_y \phi) - \partial_y(\phi^* D_x \phi)] \right. \\ &\quad \left. \pm i\frac{1}{2}\alpha^{-2} [\partial_x(s^{-1} \tilde{D}_y \tilde{S}) - \partial_y(s^{-1} \tilde{D}_x \tilde{S})] \right). \end{aligned} \quad (\text{B.2.1})$$

Since the last two terms are boundary terms which do not contribute to the total energy of the string, this leads to a lower bound on the energy per unit length

$$\mu_{string} \geq \pm (\xi g)^2 \int d^2x F_{xy}. \quad (\text{B.2.2})$$



The bound is attained by the solutions of the Bogomolnyi equations

$$\begin{aligned} (D_x \pm iD_y)\phi &= 0 \\ (\tilde{D}_x \pm i\tilde{D}_y)\tilde{S} &= 0 \\ F_{xy} \mp (1 - s^{-1} - |\phi|^2) &= 0 \end{aligned} \tag{B.2.3}$$

We will focus on cylindrically symmetric vortices, that can be described by the following ansatz:

$$\phi = f(r)e^{in\theta}, \quad s^{-1} = h^2, \quad a = m\theta, \quad A_\theta = v(r)/r, \tag{B.2.4}$$

where  $\{r, \theta\}$  are the polar coordinates in the plane transverse to the direction of the string. The ansatz for the dilaton is chosen for later convenience. It makes comparison to the semilocal case easier, and we will also see that  $h$  vanishes in various cases, thus we avoid having to deal with infinities.

With this ansatz the Bogomolnyi equations become

$$f' - f(|n| - v)/r = 0, \tag{B.2.5}$$

$$h' - \alpha^2 h^3 (|m| - v)/r = 0, \tag{B.2.6}$$

$$v'/r - (1 - f^2 - h^2) = 0, \tag{B.2.7}$$

and the total energy per unit length saturates the bound giving  $\mu_{string} = 2\pi v_\infty$ , where  $v_\infty$  is the asymptotic value of the gauge field profile function for large values of  $r$ .

The conditions (B.2.5), (B.2.6) imply the following relation between the tachyon and the dilaton:

$$1/(\alpha h)^2 = 2(|n| - |m|) \log r - 2 \log f + \kappa. \tag{B.2.8}$$

Depending on the asymptotic value of the profile functions for large values of  $r$ ,  $f_\infty$ ,  $h_\infty$  and  $v_\infty$ , we can classify the solutions to the Bogomolnyi equations in three different families. Each of them is parametrized by the integration constant  $\kappa$ .

- In the first case,

$$f_\infty = 1, \quad h_\infty = 0, \quad v_\infty = n, \tag{B.2.9}$$

the tachyon acquires a non vanishing vacuum expectation value far from the center of the string. The magnetic flux of these vortices is induced by the winding of the tachyon,  $n$ , ( $m < n$ ).

The profile function  $h(r)$  tends very slowly, (logarithmically), to zero at large  $r$ . The plots of the profile functions and the details about the asymptotics of the fields can be found in [59]. Following Blanco-Pillado et al. we call these vortices  $\phi$ -strings or tachyonic strings.

## B.2. Cosmic string solutions

---

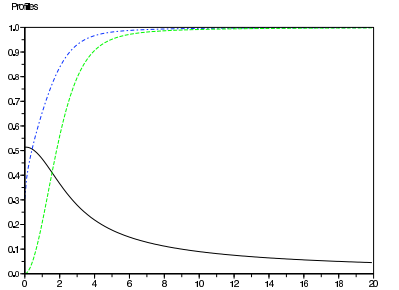


**Figure B.1** – The axion string profile functions, for  $m=1$ ,  $n=0$ ,  $a(r)$ , (upper dashed line),  $h(r)$ , (middle dashed line) and  $f(r)$ , (lower solid line), with the size of the condensate,  $f_0 = 0.51$ .

- In the second case, Fig.(B.1), the dilaton alone is responsible for compensating the D-term. The function  $h(r)$ , approaches a non vanishing constant far from the centre of the string, while the tachyon expectation value tends to zero. In this family the magnetic flux is induced by the winding of the axion,  $m$ , ( $n < m$ ).

$$f_\infty = 0 \quad h_\infty = 1 \quad v_\infty = m \quad (\text{B.2.10})$$

These vortices have been denominated *s-strings*, (or axionic). They are regular thanks to the constant Fayet-Iliopoulos term.

In the previous two families the constant  $\kappa$  has the same interpretation, each value of this parameter is associated to a particular width of the strings, as can be seen by setting:

$$k = 2(|n| - |m|) \log R \quad (\text{B.2.11})$$

In this way  $R$  gives the scale of the core radius. In the cases of  $\phi$ -strings with  $m = 0$ , and  $s$ -strings with  $n = 0$  the width of the strings, (or the core size), can be parametrized in a different way. For these particular cases, the  $\phi$ -strings and  $s$ -strings develop a condensate at the core as they grow in width. For  $\phi$ -strings the values of  $\kappa$  are in one to one correspondence with the value of the profile function  $h(r)$  at  $r = 0$ . For  $s$ -strings with  $n = 0$  each value of  $\kappa$  corresponds to a value of the profile function  $f(r)$  at the origin. Therefore, the width of the static string solutions of the BPS equations can also be parametrized in terms of  $h_0 = h(0)$  for  $\phi$ -strings, and  $f_0 = f(0)$  for  $s$ -strings.

As can be seen in (B.2.6) the derivatives of  $h$  scale as  $\alpha^2$ . In the case of the  $\phi$ -strings, varying  $\alpha$  for a fixed value of the integration constant  $\kappa$  does not change much the width of the string, but the condensate flattens. In the limit when  $\alpha$  is very small the  $\phi$ -strings are similar to a Nielsen-Olesen string. In the

case of  $s$ -strings the width of the string increases with decreasing  $\alpha$ , while the condensate does not vary much. In fact, the main effect of decreasing  $\alpha$  will be a slowing down of the dynamics.

- For strings of the third family both the tachyon and the dilaton contribute to compensate the  $D$ -term. This happens when the axion and dilaton have the same winding.

$$f_\infty^2 + h_\infty^2 = 1 \quad v_\infty = n = m \quad (\text{B.2.12})$$

In this case  $f_\infty$  and  $h_\infty$  can have any value as long as the previous relation is satisfied (B.2.12). Each particular  $f_\infty$  can be associated to a single  $\kappa$ , which means that the interpretation of this parameter is different to the previous two cases. Here the value of  $\kappa$  determines which of the fields, the dilaton or the tachyon, contributes more to compensate the Fayet-Iliopoulos term. Since it cannot be related any more to the width of the strings we will not discuss it any further.

### B.3 Numerical simulation

In [72] we analyzed numerically the response of the BPS cosmic string solutions to cylindrically symmetric perturbations. Here we will just review the main results, the technical details of the simulation can be found in [72].

The initial field configurations correspond to static cosmic string solutions of the Bogomonlyi equations, and the perturbation is chosen in order to maximize the energy absorbed by the zero mode. Actually the perturbation gives the integration constant  $\kappa$  a dependence on the radius. Since both the initial configurations and the perturbation are cylindrically symmetric, the field configuration preserves the cylindrical symmetry at all times, and therefore it can be characterized completely giving the time dependence of the profile functions  $f(r, t)$ ,  $h(r, t)$  and  $v(r, t)$ . A cylindrically symmetric perturbation is not the most general one, it does not prove stability of the  $\phi$ -strings, but it is sufficient to demonstrate the metastability of the  $s$ -strings.

## B.4. Results

---

During the simulations we kept track of a set of observables:

$$E(t) = 2\pi \int_0^{r_{cal}} dr r \mathcal{E}(r, t), \quad (\text{B.3.1})$$

$$T(t) = 2\pi \int_0^{r_{cal}} dr r \mathcal{T}(r, t), \quad (\text{B.3.2})$$

$$E_T(t) = \frac{E(t) + T(t)}{E(0) + T(0)}, \quad (\text{B.3.3})$$

$$F(t) = 2\pi \int_0^{r_{cal}} dr r B_z(r, t), \quad (\text{B.3.4})$$

$$W(t) = \frac{\int_0^{r_{cal}} dr r^2 \mathcal{E}(r, t)}{\int_0^{r_{cal}} dr r \mathcal{E}(r, t)}, \quad (\text{B.3.5})$$

where  $B_z = F_{xy}$  is the component of the magnetic field along the  $z$  direction and

$$\begin{aligned} \mathcal{E}(r, t) &= (\partial_r f)^2 + (\alpha h)^{-2} (\partial_r h)^2 + \frac{1}{2} \left( \frac{\partial_r v}{r} \right)^2 + \frac{1}{2} (1 - h^2 - f^2)^2 \\ \mathcal{T}(r, t) &= (\partial_t f)^2 + (\alpha h)^{-2} (\partial_t h)^2 + \frac{1}{2} \left( \frac{\partial_t v}{r} \right)^2. \end{aligned} \quad (\text{B.3.6})$$

The observable  $E$  is the static energy contained in a region defined by  $r < r_{cal}$ , and  $T$  the energy due to the time derivatives in the same area.  $r_{cal}$  is chosen to be much smaller than the size of the simulation box, so that the region  $r < r_{cal}$  is causally disconnected from the boundaries during the whole simulation.  $E_T$  is the total energy normalized to the initial value and  $F$  gives the magnetic flux confined in the region  $r < r_{cal}$ .

$W$  is a measure of the width of the string. In (B.3.5) the expression in the numerator is similar to the energy functional, but the extra factor  $r$  gives more weight to the energy far away from the core. Then,  $W$  increases as the energy spreads. Note that in all these expressions we have integrated over the polar angle  $\theta$  assuming cylindrical symmetry over the whole evolution. The strength of the perturbations is characterized by the value of the time derivative of the width at the beginning of the simulation:

$$\dot{W}_0 \equiv \left. \frac{\dot{W}}{W} \right|_{t=0} \Delta t, \quad (\text{B.3.7})$$

where the constant  $\Delta t$  is the time step of the simulation.

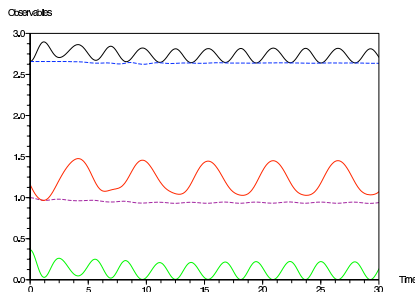


**Figure B.2** – Response of a  $\phi$ -string ( $n = 1$ ,  $m = 0$ ), with  $\alpha = 1$  and condensate size  $h_0 = 0.5$ , to a perturbation with strength  $\dot{W}_0 = -0.261$  (B.3.7). Time is measured in units proportional to the inverse of the tachyon mass,  $g\sqrt{q\xi}/20$ . From top to bottom, the plotted lines correspond to the quantities  $E$ ,  $F$ ,  $W$ ,  $E_T$  and  $T$  defined in (B.3.1-B.3.5). Except for  $W$  and  $E_T$ , the rest of the plots have been rescaled by a factor of  $1/2$  to fit in the window. The core width,  $W$ , oscillates but is constant on average showing that the zero mode is not excited.

## B.4 Results

### B.4.1 $\phi$ -strings

Fig.(B.2) shows the evolution of a  $\phi$ -string, with  $n = 1$ ,  $m = 0$  and a core size  $h_0 = 0.51$ . We show the case  $\alpha = 1$ , which is also the choice made in [59]. The perturbation applied has a strength  $\dot{W}_0 = -0.261$ , which corresponds to a 0.4% perturbation in the energy. We have plotted the observables defined in the last section as a function of time. Upper solid line represents  $E$ , the dashed line just below is the magnetic flux in  $r < r_{cal}$ , which remains almost constant. The kinetic energy,  $T$ , is represented by the bottom solid line. The dashed line at the center of the figure is the total energy. Although it can not be clearly seen in the plot, the data tell us that during the period before  $t = 12$ , a fraction of the energy is lost. This is the initial burst of radiation emitted after the perturbation. After that the system reaches a stationary state where all quantities oscillate except the magnetic flux and the total energy.

The remaining solid line in the center is the string width. As the energy contained in the region  $r \leq r_{cal}$  remains constant and the width of the vortex oscillates only around the initial value we conclude that this kind of string is stable under this perturbation. The experiment has been repeated for various types of perturbations, and for different initial widths (parametrized by  $h_0$ ), and windings, but the results are similar to the ones presented here. Nielsen-Olesen vortices react in the same way to a perturbation, as was shown in [156].

## B.4. Results

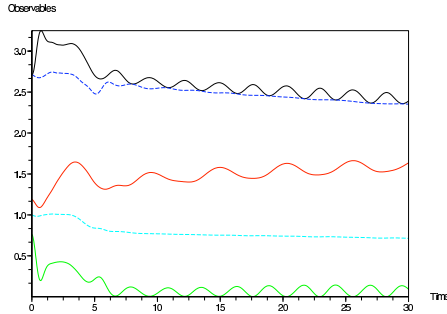


**Figure B.3** – Response of an  $s$ -string ( $n = 0$ ,  $m = 1$ ), with  $\alpha = 1$  and condensate size  $f_0 = 0.49$ , to a perturbation with strength  $\dot{W}_0 = -0.095$ . The plotted lines are, from top to bottom,  $E$ ,  $F$ ,  $W$ ,  $E_T$  and  $T$  (except for  $W$  and  $E_T$ , the rest of the plots have been rescaled by a factor of  $1/2$  to fit in the window). The core width,  $W$ , after a transient, oscillates and increases at a constant rate, the zero mode is excited in this case.

We have repeated the evolution for different values of  $\alpha$  but no qualitative change has been observed. As was mentioned before, the smaller the value of  $\alpha$ , the more similar the  $\phi$ -string is to a regular Nielsen-Olesen string, which is known to be stable.

### B.4.2 $s$ -strings

The result of applying this perturbation with a strength of  $\dot{W}_0 = -0.095$  to an  $s$ -string, with  $\alpha = 1$ , can be seen in Fig.(B.3). In this case the perturbation in energy is 2.4%. The string has windings  $n = 0$  and  $m = 1$ , and core size  $f_0 = 0.51$ . The functions plotted are the same ones that appear in Fig.(B.2). One of the most relevant features of these plots is that the magnetic flux and the total energy are decreasing with time, which implies that the energy is flowing out from the region  $r \leq r_{cal}$ , and the magnetic flux is spreading. At the same time the width of the string, ignoring the oscillatory behavior, increases at a constant rate. Before  $t = 5$  oscillations are noisy. In this period the shock wave produced by the perturbation is still inside  $r \leq r_{cal}$ .

Although the perturbation was chosen to reduce the core width, the time interval when the core is contracting cannot be seen clearly in the figures. The reason is that the contracting regime ends before the initial burst of radiation comes out from the observed region. As the system is not in a steady state yet, the data are difficult to interpret. We have chosen to show this case because the expanding regime is shown more clearly.

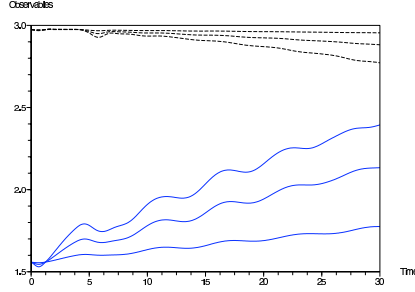


**Figure B.4** – Response of an  $n = 0$ ,  $m = 2$ ,  $\alpha = 1$   $s$ -string with a core condensate of size  $f_0 = 0.51$  to perturbations with different strengths. Dashed lines correspond to  $F$ , the strength is lowest for the top one. Solid lines represent  $W$ , the strength is highest for the top one. The strengths are:  $\dot{W}_0 = -0.004$ ,  $-0.014$  and  $-0.024$ .  $F$  is rescaled by a factor of  $1/4$ . The figure shows how the growth rate of the core increases with the perturbation strength.

Fig.(B.4) shows the effect of applying perturbations of different strengths to a  $n = 0$ ,  $m = 2$  vortex. In this case the vortex has also a condensate size of  $f_0 = 0.51$ . The strengths applied are:  $\dot{W}_0 = -0.004$ ,  $\dot{W}_0 = -0.014$  and  $\dot{W}_0 = -0.024$ .

Notice that the bigger the strength of the perturbation, the larger the fraction of magnetic flux lost through the boundary  $r = r_{cal}$ . The rate of growth of the radius also increases with the strength of the perturbation.

In Fig.(B.5) it can be seen how the rate of expansion of an  $s$ -string, ( $m = 1$ ,  $n = 0$ ), is affected by varying the value of  $\alpha$ . In this case the perturbation has been chosen to initially increase the core size  $\dot{W}_0 = 0.233 > 0$ . As we decrease  $\alpha$ , keeping the perturbation strength fixed, the rate of expansion of the string decreases. This can be understood from equation (B.3.6). The energy associated to the field  $h$  scales as the inverse of  $\alpha^2$ . Deviations from the solution to the Bogomolnyi equations cost more energy for smaller values of  $\alpha$ , thus for a fixed perturbation strength the evolution rates should decrease with  $\alpha$ . The values of alpha are:  $\alpha = 0.95$ ,  $0.94$ ,  $0.90$ .

The precision of the technique used here does not allow to obtain reliable data for values of  $\alpha$  lower than  $0.7$ , where already the evolution is so slow that it can hardly be appreciated during the time of the simulation.

## B.5. Discussion

---

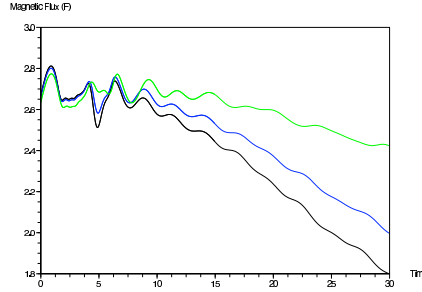


**Figure B.5** – Response of an  $n = 0$ ,  $m = 1$   $s$ -string with a core condensate of size  $f_0 = 0.51$  to a perturbation with  $\dot{W}_0 = 0.233$ . The curves represent  $F$ , the magnetic flux rescaled by a factor of  $1/4$ . From bottom to top the values of  $\alpha$  are:  $\alpha = 0.95, 0.94$  and  $0.90$ . The figure illustrates the slowing down of the core expansion with decreasing  $\alpha$

## B.5 Discussion

In order to analyze the results presented here we will use the moduli-space approximation, a semi-analytical method developed by N. Manton [33]. This technique was applied in [156] and [157] to study the dynamics of semilocal strings which, as we have mentioned previously, are closely related to the strings studied here.

According to the work by Manton, the low energy dynamics can be described restricting the Hamiltonian of the system to the solutions to the Bogomonly equations (B.2.3) with a time varying integration constant  $\kappa$ . In other words, if we substitute the static solutions to the Bogomonly equation (B.2.4) into the energy functional with  $\kappa$  promoted to be time dependent, we obtain an effective Hamiltonian for  $\kappa(t)$ . The evolution of  $\kappa(t)$  obtained from this effective Hamiltonian approximately characterizes the evolution of the system at low energies.

For convenience we rewrite  $\kappa$  as

$$\kappa = 2(|n| - |m|) \log R \quad (\text{B.5.1})$$

and we study the dynamics of the parameter  $R$  which represents the width of the strings. The static cosmic string solutions of the Bogomonly equations can be written as functions of this parameter:

$$f = f(r, R), \quad h = h(r, R), \quad v = v(r, R), \quad (\text{B.5.2})$$



and promoting  $R$  to time dependent we have:

$$\dot{f} = \partial_R f \dot{R}, \quad \dot{h} = \partial_R h \dot{R}, \quad \dot{v} = \partial_{Rv} \dot{R}. \quad (\text{B.5.3})$$

Substituting this ansatz into the energy functional associated to the lagrangian B.1.7 we find that the total energy of the string for time dependent (and homogeneous) parameter  $R(t)$  reads:

$$(\xi g)^{-2} \mu_{string} = 2\pi \max\{|n|, |m|\} + \delta E_{pert}, \quad (\text{B.5.4})$$

where the energy of the perturbation is given by:

$$\delta E_{pert} = \int dr r \left( (\partial_R f)^2 + \frac{1}{\alpha^2} \left( \frac{\partial_R h}{h} \right)^2 + \frac{(\partial_{Rv})^2}{2r} \right) \dot{R}^2. \quad (\text{B.5.5})$$

Note that, since the energy of the static string configuration stays the same for every value of  $R$ , the only new contribution to the energy due to the time dependence of  $R(t)$  comes from the kinetic terms.

For  $\phi$ -strings with  $n = 1$  and  $m = 0$  the asymptotic behavior of the profile functions for  $r \rightarrow \infty$  is [59]:

$$f_\infty = 1, \quad h_\infty \sim \log(r/R)^{-1/2} \quad v_\infty = |n|. \quad (\text{B.5.6})$$

substituting this in the expression we just derived for the energy per unit length of the perturbation (B.5.5) we find that it has a divergent contribution of the form:

$$\delta E_{pert} \sim \int_{r_c}^{\Lambda} dr \frac{r}{\log(r)^2} \dot{R}^2 \sim \frac{\Lambda^2}{(\log \Lambda)^2} \dot{R}^2, \quad (\text{B.5.7})$$

where  $\Lambda$  is a cutoff, and  $r_c$  is the core radius of the string. Thus the amount of energy needed in order to excite the zero mode in a cylinder of radius  $\Lambda$  centered on the string scales almost as  $\Lambda^2$ . In other words given an perturbation of energy  $\delta E_{pert}$ , the size of the region where the zero mode can be excited scales approximately as:

$$\Lambda \sim (\delta E_{pert})^{1/2}. \quad (\text{B.5.8})$$

Clearly any finite energy perturbation can not excite the zero mode everywhere in space, since this would require an infinite energy. If such a perturbation is localized around the core of the string it is not expected to propagate further away than a distance  $\Lambda$  from the string center. This is consistent with the observed results shown in figure B.2, which indicates that perturbing the static solution leads to oscillations in the string width and not to the spread of the magnetic flux.

It would seem that the infinity we have obtained for the kinetic energy of the perturbations is a result of promoting the parameter  $R$  to time dependent

## B.5. Discussion

---

while keeping it homogeneous. However, a perturbation  $R(t)$  independent of the coordinates does not necessarily imply that the profile functions are modified everywhere in space. Indeed, the profile functions  $f(r)$ ,  $h(r)$  and  $v(r)$  are perturbed only for those values of  $r$  such that  $\partial_R f(r) \neq 0$ ,  $\partial_R h(r) \neq 0$  and  $\partial_R v(r) \neq 0$  respectively. As we shall see in the case of  $s$ -strings, if these derivative decay sufficiently fast for  $r \rightarrow \infty$ , it is still possible to obtain finite results for the energy of the perturbations without introducing a space dependence on the parameter  $R$ .

The asymptotic behavior of  $s$ -strings is given by:

$$f_\infty \sim (r/R)^{|n|-|m|}, \quad h_\infty = 1, \quad v_\infty = |m|, \quad (\text{B.5.9})$$

and therefore, substituting into (B.5.5), we see that the perturbation has an energy per unit length of the form

$$\delta E_{pert} \sim \int_{r_c}^{\Lambda} dr r \sim r^{2(|n|-|m|)} \dot{R}^2. \quad (\text{B.5.10})$$

In particular, for the case studied here  $m = 1$  and  $n = 0$ :

$$\delta E_{pert} \sim \int_{r_c}^{\Lambda} \frac{dr}{r} \dot{R}^2 \sim \log \Lambda \dot{R}^2. \quad (\text{B.5.11})$$

Therefore, a perturbation of energy  $\delta E_{pert}$  can only excite the zero mode in a cylinder centered on the string of radius  $\Lambda$ , which scales as

$$\Lambda \sim \exp(\delta E_{pert}). \quad (\text{B.5.12})$$

This analysis implies that an infinite energy is also needed in the case of  $s$ -strings in order to excite the zero mode everywhere in space. However the energy only scales logarithmically, in contrast with the almost quadratic divergence that appeared in the case of  $\phi$ -strings. In a cosmological setting the string network has a natural length scale which acts as a cutoff, the typical inter-string distance. Due to this mild dependence on the cutoff, the perturbations inherent to any cosmological setting might be able to excite the zero mode, leading to the growth of the radius of the string and the eventual dilution of the magnetic flux. This is precisely confirmed in our simulations, where the cutoff is given by the size of the simulation box. As we have shown in figure B.3, perturbations with small amount of energy compared to the total energy of the string can excite the zero mode leading to the dilution of the magnetic flux. Note that for  $|n| - |m| < -1$  the integral (B.5.10) becomes finite, and therefore any finite energy perturbation is enough to induce a growth of the parameter  $R$  everywhere in space.

This analysis is closely related to the discussion in section 7.5.3, where we consider the stability of cosmic string solutions in a  $\mathcal{N} = 2$  supergravity model.

The model admits a family of string solutions parametrized by the value of one of the fields, the axio-dilaton  $S$ . In particular the radius of the string scales as the imaginary part of  $S$ . The imaginary part of the axio-dilaton  $\text{Im } S = -e^\rho$  has a standard kinetic term of the form (7.4.6):

$$\int dr r \partial_\mu \rho \partial^\mu \rho, \tag{B.5.13}$$

thus, in order to study the excitability of the zero mode associated to the value of  $\rho$ , we promote it to time dependent function. The time dependence of  $\rho$  introduces a contribution to the total energy of the configuration:

$$\delta E_{\text{pert}} \sim \int_{r_s}^\Lambda dr r \dot{\rho}^2 \sim \Lambda^2 \dot{\rho}^2, \tag{B.5.14}$$

which scales with the cutoff in the same way as the perturbation of a  $\phi$ -string. This suggests that this zero mode will not be excited by any finite energy perturbation, as was anticipated in section 7.5.3, and thus the radius of the cosmic string will not tend to grow in a cosmological context.